

Quantifying the Hydrodynamic Stress for Bioprocesses

Umut Kaya^{*†§} Srikanth Gopireddy[†] Nora Urbanetz[†]
Diana Kreitmayer[†] Eva Gutheil[‡] Ingmar Nopens[§]
Jan Verwaeren[§]

April 25, 2023

Abstract

Hydrodynamic stress is an influential physical parameter for various bioprocesses, affecting the performance and viability of the living organisms. However, different approaches are in use in various computational and experimental studies to calculate this parameter (including its normal and shear subcomponents) from velocity fields without a consensus on which one is the most representative of its effect on living cells. In this letter, we investigate these different methods with clear definitions and provide our suggested approach which relies on the principal stress values providing a maximal distinction between the shear and normal components. Furthermore, a numerical comparison is presented using the computational fluid dynamics simulation of a stirred and sparged bioreactor. It is demonstrated that for this specific bioreactor, some of these methods exhibit quite similar patterns throughout the bioreactor—therefore can be considered equivalent—, whereas some of them differ significantly.

Keywords: CFD, Bioprocess, Hydrodynamic Stress, Normal and Shear Stresses ■

*Corresponding author. umut.kaya@ugent.be

[†]Daiichi-Sankyo Europe GmbH, 85276 Pfaffenhofen an der Ilm, Germany

[‡]Interdisciplinary Center for Scientific Computing, Heidelberg University, 69120 Heidelberg, Germany

[§]Department of Data Analysis and Mathematical Modelling, Ghent University, Coupure Links 653, 9000 Gent, Belgium

1 Introduction

Utilizing a living organism inside a controlled liquid environment is a common aspect of bioprocess technologies. In this letter, we investigate one of the most important physical factors affecting cell viability and productivity, namely the hydrodynamic stress, using a computational fluid dynamics simulation of a stirred and sparged tank bioreactor. The hydrodynamic stress can deform the cells, physically damage them, and inhibit their growth and viability; therefore, it is a critical parameter to monitor and control when studying different bioreactor geometries and scales¹⁻⁵. With an adequate stirrer rotational speed, a well-mixed and homogeneous cell culture medium can be achieved. However, this increased mixing/homogeneity comes at the cost of increased hydrodynamic stress, which in return will reduce cell viability and growth⁶. Besides its effect on living cells, hydrodynamic stress exerted at various stages of bioprocesses (e.g. centrifugation, ultrafiltration, etc.), can also influence the structure of protein molecules⁷ (for a bioprocess-focused review, see Schuegerl et al.³). The hydrodynamic stress not only affects cells in bioprocesses and other production methods but also in other settings such as cancer cells in the blood vessels^{8,9}, intestinal cells¹⁰, and dinoflagellate bioluminescence¹¹.

Experimental studies suggest that the normal and shear components of the hydrodynamic stress differ in the way they affect cells inside a bioreactor^{1,3}. It was reported that both shear and normal flows can result in apoptotic cell deaths at comparable stress levels¹. However, it was also reported that shear flows cause cell membrane damage at a lower stress compared to normal flows¹. Although the hydrodynamic stress is frequently used in various studies, the definition behind the relevant terms (such as strain, hydrodynamic stress, shear stress and normal stress) are not always explicit, and there is no consensus on how to calculate them. It is not always explicitly stated how the normal and shear components of hydrodynamic stress are calculated^{12,13}; in certain studies authors rely on theoretical simplifications (e.g., considering only 1D or 2D flows) to do approximate formula-based calculations¹⁴⁻¹⁶. It is common to see that in many studies the term shear stress is used interchangeably with the total hydrodynamic stress without actually highlighting the normal/shear distinction¹⁷. As will be discussed in this work, there are differences in the calculation of these terms in

respective studies. Therefore, our aim is (i) to clarify how these terms are defined and can be calculated from a numerical point of view, and (ii) illustrate how the different ways of calculating these terms can lead to different results when applied to CFD simulation data of a specific bioreactor.

Although in some papers hydrodynamic stress is also referred to as shear stress without a clear distinction why, one of the main reasons is the nature of their experimental methods which uses devices such as capillary/microfluidic or rotational flow^{7,18,19}. Depending on the work, the term shear stress might actually correspond to the total hydrodynamic stress without implying any normal and shear distinction (i.e., the magnitude that includes both normal and shear components). A common experimental approach is to use stress sensitive poly(methyl methacrylate) (PMMA) aggregates to indirectly quantify the maximum hydrodynamic stress levels in a setup²⁰.

Computational fluid dynamics (CFD) simulations allow local hydrodynamics to be calculated for different stirrer speeds and tank geometries. As opposed to experimental approaches hydrodynamic stress can be calculated directly from the velocity fields (and turbulence parameters) using first principles. A typical monoclonal antibody production can hold $5 - 30 \times 10^6$ cells per ml⁶. Considering a simulation mesh of 2×10^6 voxels for a 1 L tank, each voxel/cell in a simulation mesh can hold $2.5 - 15 \times 10^3$ cells. This means that the resolution of a typical CFD simulation is far from resolving the flow events at cell scale, and the calculated values should be interpreted as average values influencing thousands of cells.

There are various ways to calculate the hydrodynamic stress using CFD simulations. The most common way is to use the magnitude of the stress tensor. However, this method cannot differentiate between the shear and normal components. In order to make this distinction, one way is to rotate the stress tensor into the average flow direction²¹, however this method does not ensure that this specific frame of reference is the one maximizing the calculated shear stress.

In this study, a third way that allows a distinction between the shear and normal components using the principal stresses is proposed. The principal stresses correspond to the eigenvalues of the stress tensor; therefore, they are independent of the frame of reference selected for the calculations. Moreover, we define and explain how these scalar values are

computed from a CFD simulation. Since such CFD simulations cannot fully resolve the turbulent fluctuations, in addition to the fluid flow based approaches, we further elaborate on how the modeled turbulent energy dissipation rate can be utilized to quantify the turbulent hydrodynamic stress. Lastly, even though it is trivial to see that these quantities are affected differently by the components of hydrodynamic stress—and therefore quantify different phenomena—, we use simulation results of a (previously) validated CFD model of a bioreactor to show the relationships between these quantities in a practical industrial application²².

2 Preliminaries

In this section a minimal set of equations and definitions that constitutes the relation between stress, strain and deformation are given.

Stress is defined as the force per unit area acting on a surface. For a given frame of reference the stress on an infinitesimal cubic volume element aligned with the coordinate axes can be denoted by T_{ij} , where the indices $i, j \in \{1, 2, 3\}$ represent the stress components; i indicating the direction of the force, j indicating the side that the force is acting upon (see Figure 1a for a visual depiction). The opposite-sided faces of the infinitesimal volume element have equal stress values in opposite directions due to Newton’s 3rd law (also called Cauchy’s fundamental lemma), in other words the tensor is symmetric, $T_{ij} = T_{ji}$.

When the frame of reference changes, T_{ij} transforms as a tensor, hence it is also named (Cauchy) stress tensor²³:

$$\mathbf{T}' = \mathbf{R}\mathbf{T}\mathbf{R}^\top, \tag{1}$$

where \mathbf{R} is a rotation matrix. A real matrix, $\mathbf{R} \in \mathbb{R}^{n \times n}$, is called a rotation matrix if it has a unit determinant, $\det(\mathbf{R}) = 1$, and is orthogonal, $\mathbf{R}^\top = \mathbf{R}^{-1}$.

Forces that are parallel to the surface are called shear, and those that are perpendicular are called normal. That is, the diagonal terms of the stress tensor T_{ii} correspond to normal stresses and non-diagonal terms $T_{ij, i \neq j}$ correspond to shear stresses. Note that as the frame of reference changes (Eq. 1), the shear and normal components of stress would change as well.

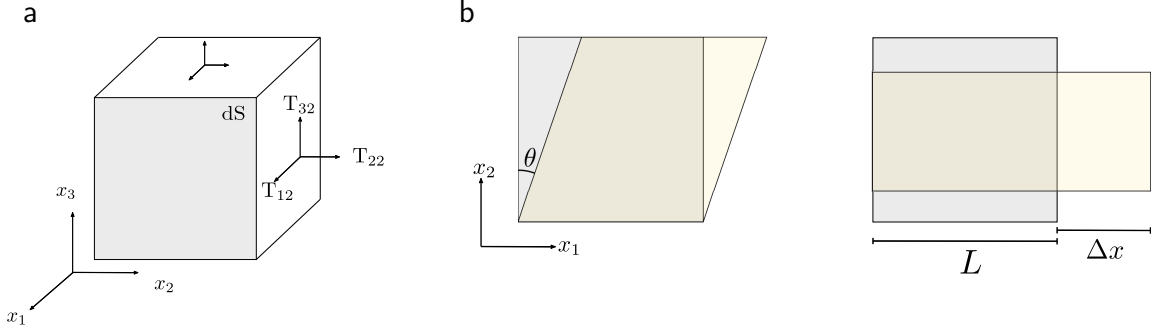


Figure 1: (a) Stress tensor components for a cubic volume element. (b) (Left) Pure shear deformation in x_1 direction and (Right) pure stretching in x_1 direction for a 2D body.

The relationship between the stress tensor and the fluid flow can be established using the first order deformations, $\frac{\partial u_i}{\partial x_j}$, where u is the velocity field. Such deformations can be represented by two components, named normal (or stretching or extensional) and shear strain. Shear strain is defined by the amount of tangential movement. For the deformed body in Figure 1b, shear strain is defined as $\gamma = \tan \theta$ for pure shear, and normal strain is defined as $\frac{\Delta x}{L}$.

For an infinitesimal fluid volume with velocity field u , the symmetric part of the deformation tensor, $\frac{\partial u_i}{\partial x_j}$ is called rate of strain (deformation) tensor—in short, strain rate—denoted by D_{ij} , and the antisymmetric (skew) part is called vorticity tensor denoted by E_{ij} ²⁴:

$$D_{ij} = \frac{1}{2} \left(\frac{\partial u_i}{\partial x_j} + \frac{\partial u_j}{\partial x_i} \right), \quad E_{ij} = \frac{1}{2} \left(\frac{\partial u_i}{\partial x_j} - \frac{\partial u_j}{\partial x_i} \right). \quad (2)$$

The vorticity E_{ij} does not deform the volume that it acts upon, but only rotates it, therefore it does not cause any strain²³.

For a given frame of reference the diagonal components of the strain rate tensor (D_{ij} , where $i = j$) correspond to normal/stretching deformations directed towards the corresponding axes and off-diagonal components (D_{ij} , where $i \neq j$) correspond to shear deformations parallel to corresponding axes.

For a linearly viscous (Newtonian), isotropic, and incompressible fluid the following equation holds²⁴:

$$T_{ij} = 2\mu D_{ij} - p\delta_{ij}, \quad (3)$$

where μ is called viscosity, p is pressure.

The first term (hydrodynamic stress without the hydrostatic pressure) is referred to as the viscous stress tensor (or deviatoric stress tensor), which is equivalent to the strain rate tensor up to a constant and denoted as σ . For the rest of the work, we will refer to this value as “stress” unless explicitly specified otherwise.

Note that the coefficient in the definition of the rate of strain tensor might be different depending on the textbook. The rate of strain tensor is sometimes defined without the 1/2 factor in Eq. 2, hence the magnitudes of the tensors have different definitions as well to match the given definitions²⁵.

3 Hydrodynamic Stress Calculations

The mechanism behind how hydrodynamic stress affects living cells is an active research field. It is often observed that negative effects appear once the hydrodynamic stress passes a threshold, and the normal and shear components of hydrodynamic stress affect cell viability differently. Nevertheless, there is no consensus on how to derive a scalar quantity from the aforementioned tensors that describes these normal and shear components. We provide three hydrodynamic stress parameters that can be calculated from the velocity field. In addition, we explain how the turbulent hydrodynamic stress can be quantified.

1) **Magnitude of the stress tensor.** The magnitude of the (viscous) stress tensor is defined by the following norm:

$$\|\sigma\| = \sqrt{\frac{1}{2}\text{Tr}(\sigma\sigma^T)} = \mu\sqrt{2\text{Tr}(\mathbb{D}\mathbb{D}^T)} \quad (4)$$

As mentioned in the previous section the coefficient in the strain rate definition varies between studies. It is common to refer to $\tau = \sqrt{2\text{Tr}(\mathbb{D}\mathbb{D}^T)}$ as the strain rate magnitude, so that it gives the magnitude of the stress when multiplied with μ .

The energy dissipation rate is tightly connected to these quantities and frequently used to characterize the hydrodynamics of bioreactors through CFD simulations²⁶. It is defined as

$$\epsilon = 2\nu\text{Tr}(\mathbb{D}\mathbb{D}^T), \quad (5)$$

where $\nu = \mu/\rho$ is the kinematic viscosity and ρ is density²⁷.

Regardless of the used form, the magnitude of the stress represents the total force exerted on a unit volume element, therefore it is a viable approach to examine the effects of the hydrodynamic stress on cells. Various studies use this quantity and obtain it either through experimental and/or CFD studies of bioreactors²⁸.

Given a frame of reference, the diagonal and non-diagonal values can be used to differentiate normal and shear stresses^{29,30}. However, the magnitudes of the shear and normal stresses depend on this—rather arbitrary—frame of reference and would give different results for different frame of references (although the total stress magnitude is invariant under rotations). As mentioned before the stress tensor becomes diagonal in the frame of reference defined by the principal stress axes. Moreover, for a traceless tensor (like the viscous stress and strain rate tensors), a direction where the diagonal terms are all zero can always be found. Therefore, the maximum values for these shear and normal stress magnitudes would always correspond to the initial magnitude itself, as the magnitude of a tensor is invariant under rotations. That is, this method cannot be reliably used to differentiate the normal and shear components of hydrodynamic stress.

2) **Normal and shear stresses in the average velocity frame of reference.** In this method the average velocity direction is selected as the frame of reference and the normal and shear components are calculated by rotating the stress tensor on this frame of reference. Kaiser et al.³¹ and Wollny²¹ refer to Langer and Deppe³² in order to argue how and why these components need to be separated for a better assessment of stress on cells. In short, the frame of reference is transformed so that the first axis is aligned with the average velocity direction. In this new frame of reference, the stress tensor can be calculated by rotating the initial stress tensor using axis transformation, i.e. $\sigma' = R\sigma R^T$. See Wollny²¹ for the details of the calculation; Werner et al.³³ and Kaiser³⁴ as further studies using this approach.

Although intuitively this may seem to be a reasonable approach, it is unclear why the definition of the shear and normal components of the stress depends on the average velocity direction. As a counter example, consider a volume in a stationary point in the volume with non-zero shear force, with this method one cannot complete the calculations since the average velocity is zero. Moreover, this average velocity direction often does not correspond to the direction leading to the maximum normal or shear deformations. Therefore, this approach

is not optimal for distinguishing the normal and shear strain. As a result, researchers who believe that shear stress is the main determinant for cell viability would systematically underestimate the maximal shear strain a cell faces when using this method.

3) **Principal stress components.** Instead of using a specific frame of reference as in the previous method, finding the direction which maximizes the relevant deformation is a valuable alternative. This maximization is quite straightforward using the invariants of the stress tensors, called principal stresses (or strain rates). Principal stresses are well examined quantities in various textbooks³⁵.

For any symmetric tensor, one can always find a rotation matrix R which diagonalizes the tensor²³. That is, we can always rotate our frame of reference where $\sigma' = R\sigma R^T$ is diagonal in this rotated frame, i.e. $\sigma'_{ij} = \lambda_i \delta_{ij}$. These ordered eigenvalues are called principal stresses:

$$\begin{bmatrix} \sigma_1 & 0 & 0 \\ 0 & \sigma_2 & 0 \\ 0 & 0 & \sigma_3 \end{bmatrix}, \text{ where } \begin{cases} \sigma_1 = \max\{\lambda_1, \lambda_2, \lambda_3\}, \\ \sigma_3 = \min\{\lambda_1, \lambda_2, \lambda_3\}, \\ \sigma_2 = \text{tr}(\sigma) - \sigma_1 - \sigma_3 \end{cases} \quad (6)$$

The eigenvectors corresponding to these eigenvalues are called principal directions, and they form the principal coordinate frame. Note that in this frame of reference the deformations are purely normal, meaning the highest absolute eigenvalue corresponds to the largest normal deformation. There are studies using this eigenvalue to characterize the stress in bioreactors^{1,36}.

For an arbitrary surface/direction, the shear and normal components of the stress can be found using the Mohr's stress representation plane³⁷. The maximum shear stress can be calculated using the principal stresses:

$$\sigma_{\text{shear, max}} = \frac{1}{2} (\sigma_1 - \sigma_3). \quad (7)$$

For two dimensions the maximum shear direction is the 45° angle between maximum and minimum principal stress directions (see Figure 2). In general, the following values are called principal shear stresses (they correspond to the shear stress value on the octahedral plane):

$$\sigma_{\text{shear,1}} = \frac{1}{2} (\sigma_1 - \sigma_3), \sigma_{\text{shear,2}} = \frac{1}{2} (\sigma_1 - \sigma_2), \sigma_{\text{shear,3}} = \frac{1}{2} (\sigma_2 - \sigma_3).$$

By definition, σ_1 and $\sigma_{\text{shear,max}}$ do not depend on a single frame of reference as opposed to the second method, instead they represent the highest possible deformations given a certain stress.

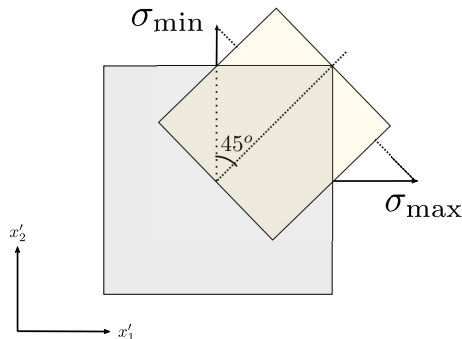


Figure 2: Visual explanation of the maximum shear direction, which is 45° between maximum and minimum principal stress directions.

4) Quantifying the effect of turbulence.

In the previous paragraphs, we described three different methods that allow the calculation of the relevant hydrodynamic stress parameters from velocity fields. However, in real-world applications, even for lab-scale reactors, it is not feasible to measure (e.g., via Laser Doppler Velocimetry, or Particle Imaging Velocimetry) or calculate a high resolution velocity field (both spatially and temporally) that is sufficient to resolve the turbulent flows affecting the living organisms. In particular, the CFD studies of bioprocesses cannot use a direct numerical simulation (DNS), but instead they use turbulence models such as Reynolds-averaged Navier-Stokes (RANS), large eddy simulation (LES), and Reynolds stress equation model (RSM). These models separate the mean and the fluctuating parts of the velocity field and model the turbulent effects of the fluctuating part via additional Reynold stress terms in the Navier-Stokes (NS) equations.

These turbulence models can be used to estimate the hydrodynamic stress effect of the turbulence on the living cells. Even though quantifying the effect of turbulence—for all turbulence models—is not the major goal of this letter, we highlight the following two important points: (i) deformation tensor based approaches cannot be readily applied to turbulence models (see below), and (ii) a simplified analysis can assume that turbulent (fluctuating) and mean hydrodynamic stress parameters can be studied separately, and their effects can be

added.

In the CFD analysis part of this study we used the k- ϵ turbulence model, which is shown to be effective in predicting the hydrodynamic properties in this and similar setups²². In the k- ϵ model (also in many other turbulence models) turbulent kinetic energy is assumed to be isotropic, therefore it cannot predict any non-isotropic deformations coming from turbulent forces. This means that the turbulent hydrodynamic stress parameters calculated from the model parameters should only be used in magnitudes, as there is no mechanistic way to distinguish the normal and shear components as in the other methods without further assumptions. In some studies further physical assumptions are made to find an estimate normal and shear components of the total stress magnitude^{38,39}, however the validity of these approaches has not been studied in similar—bioprocess—setups.

The turbulent energy dissipation rate can be used to characterize the various bioreactors in order to quantify the corresponding hydrodynamic stress it induces on the cells⁵. Besides its usage in CFD studies, it is also used in experimental studies⁴⁰. The total energy dissipation can be determined by the mean and turbulent components as

$$\epsilon_{\text{total}} = \epsilon + \epsilon_{\text{turb}} = 2(\nu + \nu_{\text{turb}})\text{Tr}(\mathbf{D}\mathbf{D}^T), \quad (8)$$

where ν_{turb} is the turbulent kinematic viscosity and \mathbf{D} corresponds to strain rate of the mean flow. Similar to Equation 5, one can calculate the turbulent strain rate magnitude by

$$\tau_{\text{turb}} = \frac{\epsilon_{\text{turb}}}{\nu}. \quad (9)$$

It is important to highlight that turbulent flows are inherently chaotic consisting of small scale fluctuations, and the turbulence models aim to model the effects of these turbulent flows by making certain physical assumptions. In this case, turbulent energy dissipation rate needs to be treated as a random variable with a probability distribution. The instantaneous energy dissipation rate, therefore, might be much higher or lower at a given point. See Morshed et al., for a detailed discussion (with a focus on turbulent blood flows)⁴¹.

4 Results and Discussions

In the previous section, three methods that allow to calculate hydrodynamic stress were described. In order to test and compare these hydrodynamic stress parameters, we applied them to a CFD simulation of a stirred and sparged bioreactor. The bioreactor is a 3 L Mobius CellReady bioreactor (Merck KGaA, Darmstadt, Germany) with a microporous sparger (gas flow rate at 0.02 L/min) and a marine-blade impeller with three blades (rotating at 250 rpm). See Figure 3 for a visual illustration of the setup. This simulation setup has previously been developed in a study and validated with experimental measurements for various physical quantities (mixing time and specific oxygen mass transfer coefficient)²². The CFD modeling assumptions and choices—that are also made in this work—closely follow the previous work and are known to be effective in predicting the hydrodynamic properties of similar bioreactors^{42,43}.

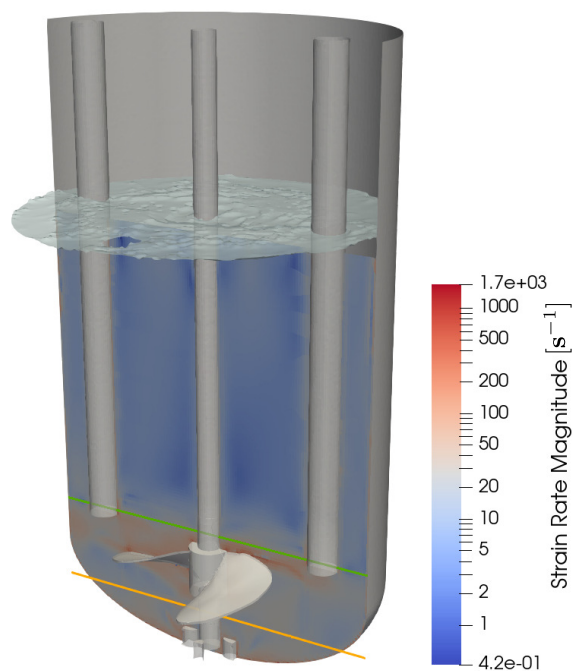


Figure 3: Snapshot of the strain rate magnitude of the bioreactor at $t = 1$ s. The green and orange lines above and below the impeller denote the path used for the comparison plots.

Figure 4 shows a comparison between different hydrodynamic stress parameters over two

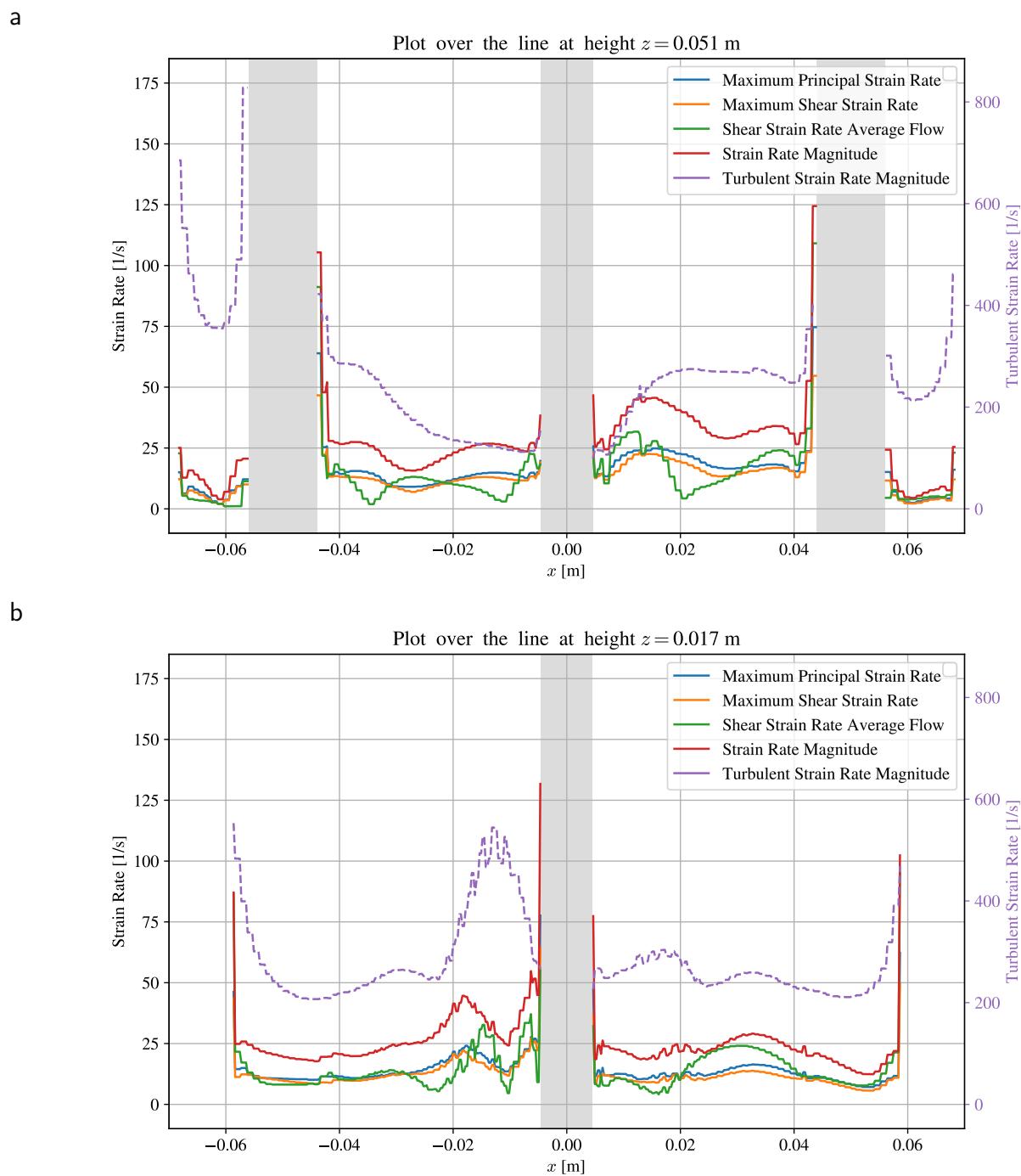


Figure 4: Comparison of different hydrodynamic stress parameters over the lines at different heights of the bioreactor. The turbulent strain rate magnitude is indicated with a dashed purple line and has a second y-axis due to scale difference. The location of the impeller shaft and the measurement probes are shaded in gray.

Table 1: The Spearman (lower triangle values) and Kendall (upper triangle values) correlations for the relevant hydrodynamic stress parameters.

	Kendall	Strain Rate Magnitude	Maximum Shear Strain Rate	Shear Strain Rate Average Flow	Maximum Principal Strain Rate
Spearman					
Strain Rate Magnitude		1.000000	0.980557	0.749887	0.966495
Maximum Shear Strain Rate		0.999257	1.000000	0.750579	0.948348
Shear Strain Rate Average Flow		0.898023	0.898397	1.000000	0.745956
Maximum Principal Strain Rate		0.998308	0.995853	0.896303	1.000000

transects through the bioreactor. The first transect is positioned above the impeller and the second transect is placed beneath the impeller. They intersect various walls, such as impeller shaft and measurement probes, as indicated with green and orange lines in Figure 3. It can be observed that all three methods provide different hydrodynamic stress patterns over the sample line. Assuming that the cell viability and growth is abruptly affected after crossing a threshold in the stress value², these different approaches would give different numerical results. Even though these quantities are different numerically, it can be observed that some of them exhibit quite similar patterns. To quantify this similarity the Spearman and Kendall correlations are calculated throughout the bioreactor (Table 1). If a—possibly nonlinear—monotonic relation exists among two datasets, both of these correlation measures give values close to 1. Kendall correlation is considered to be more robust against outliers. The very high correlations between the strain rate magnitude and the values from the principal strain rates suggest that thresholds found for one quantity can be transformed in a corresponding threshold for another quantity that will generally lead to a highly similar partitioning of a bioreactor in regions that are harmful or not for cell viability. Moreover, these results also suggest that for this setup the maximum values that normal and shear strain rate take are very close both in magnitude and in terms of correlation; therefore, both normal and shear forces could play an important role in the cell viability. On the other hand, the method with the average velocity frame of reference has a different behavior as opposed to the other methods, which is reflected in Figure 4, and in Table 1.

Since experimental studies suggest that the detrimental effects of stress become prominent

only after it passes a certain threshold, using the magnitude might be misleading instead using “one-dimensional” values like principal stress components can be preferred. Moreover, most formula-based approaches are also not magnitude based, therefore comparing various studies would be more reliable with these approaches.

When comparing different stress and strain thresholds from various studies, there are a few points that need to be considered. Firstly, one needs to consider how viscosity plays a role in cell damage and decide whether it is the force on a surface (quantified by stress) or the deformation (quantified by strain rate) that adversely impacts the cell viability or its production efficiency. Stress values could take much different values for the same strain—thus same deformation—, so simply comparing these values among different studies might be misleading. Secondly, as discussed in this work, some approaches use magnitude as a sum of various strain components, and the others use single values, comparing these values might cause wrong implications for the setup under investigation. This argument also extends to the formulas determined by either theoretical assumptions or experimental results. Lastly, we would like to stress once again (see Section 2) that the selected coefficient in the definition of stress-strain relation (and their magnitudes), might be different from study to study depending on the definition that authors have selected (or that the software used). Therefore, corresponding values might need to be scaled up or down by a factor of two, before comparing them among different studies.

If the normal and shear distinction of the hydrodynamic stress is not crucial to the process under consideration, the magnitude of the stress tensor is the most straightforward way to quantify this parameter. However, if a distinction is necessary, using the principal stress components to calculate the maximum normal and shear is the most suitable way to achieve this distinction properly.

As mentioned before, in this work, we used the k - ϵ model to calculate the turbulent hydrodynamic parameters. The turbulent strain rate magnitude calculated from the modeled turbulent kinetic energy is found to be on average 9.7 times larger than the mean flow strain rate magnitude in this setup, which is also reflected in Figures 4 and 5. But the maximum value they take throughout the reactor is found to be close to each other (turbulent: 8983.6 s^{-1} , mean flow: 7863.3 s^{-1}). As discussed before, the turbulent strain rate magnitude needs

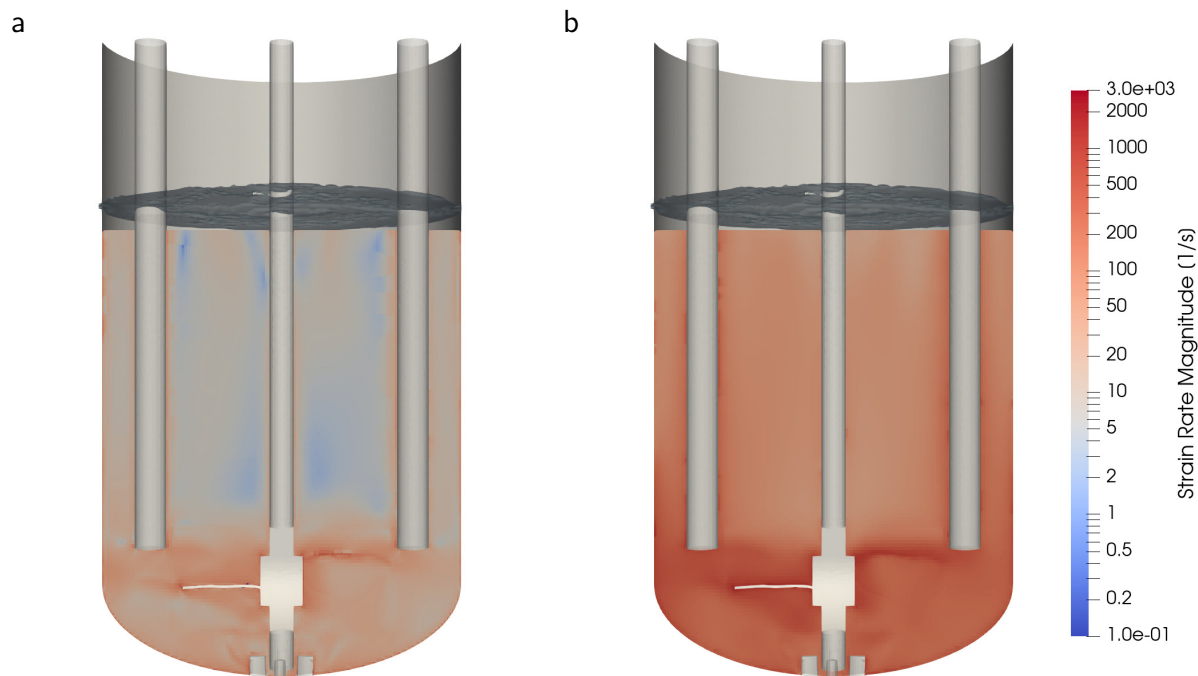


Figure 5: Strain rate magnitude calculated for the mean (left) and turbulent flows (right).

to be considered as a potential additional source of deformation in addition to the mean flow based calculations, therefore it is not added to the correlation analysis. Although theoretically these quantities represent the same physical parameters, their potential meaning in terms of small scale deformations—in a bioprocesses—is different. The strain rate calculated (or measured) from the mean flow, exerts deformation on a volume element as explained in Section 2. However, whether the turbulent strain rate calculated from the turbulent energy dissipation would deform the cells in the same mechanism or not is an open question. As we are not resolving the turbulent eddies directly, we need to consider further aspects in order to address this issue. One possible aspect that is frequently raised in similar studies is the Kolmogorov length scale. This parameter represents the size of the smallest turbulent eddies, below which the turbulent energy is fully dissipated into heat; and therefore argued to be important when it is close to the size of the cells inside a bioreactor. In this setup we observed that the minimum Kolmogorov length scale is $11.14\ \mu\text{m}$ and comparable to the mammalian cell size ($10\text{-}20\ \mu\text{m}$), whereas its average value is considerably larger ($104.2\ \mu\text{m}$). This indicates that at highly turbulent regions, the strain effects of turbulence calculated

from the turbulent energy dissipation rate should be taken into account.

5 Conclusion

In this letter, we provided clear definitions for the most common hydrodynamic stress parameters and a numerical comparison using the CFD simulation of a bioreactor.

A properly calculated hydrodynamic stress during the design phase will ensure a reliable process for different geometries and scales. We showed that different hydrodynamic stress properties in certain cases can result in different results in the bioreactor, therefore has to be treated properly. If the velocity data is acquired via CFD simulations both mean and fluctuating velocities need to be considered. For the mean velocity field, the principal stress based calculations allows a maximal distinction between the shear and normal components. For the fluctuating velocity field, the turbulent kinetic energy dissipation rate can be used to calculate the hydrodynamic stress magnitude. Assuming that the isotropicity argument of the turbulence models is valid, such distinction between normal and shear components is not relevant for the turbulent fluctuations.

The CFD simulation that we used is representative of the typical bioreactor-level simulations for similar studies. In order to better address the hydrodynamic stress calculations, several improvements can be made on the simulation approach so that more granular fluctuating velocities can be resolved. First, using a large eddy simulation (LES) can provide more resolved velocity at smaller scales, which could be used to further investigate the hydrodynamic stress effects of turbulent flows. Second, the simulation can be improved by using a finer mesh focusing only a portion of the bioreactor geometry, in particular the impeller. This would allow for a more accurate calculation of the hydrodynamic stress around the impeller, which is the most critical region in the bioreactor. Supported with further the wet-lab experiments these improved CFD simulations may give further insight about the hydrodynamic stress in bioreactors.

Especially in experimental studies without the CFD analysis, the definitions tend to differ among different studies, since they frequently rely on certain physical assumptions and are calculated with formulas that are based on theoretical simplifications. For those studies

where the full hydrodynamic stress tensor is not available, it is difficult—if not impossible—to compare different studies. Therefore, for a proper identification of the relevant critical parameters of a (bio)process, we suggest a CFD analysis of the flow would give proper insights to the designer. In this aspect, we believe this work would provide a guidance to those experimental studies in selecting the most relevant hydrodynamic stress parameter affecting the living cells.

6 Acknowledgements

The computational resources (Stevin Supercomputer Infrastructure) and services used in this work were provided by the VSC (Flemish Supercomputer Center), funded by Ghent University, FWO, and the Flemish Government – department EWI.

This work was supported by Daiichi Sankyo Europe GmbH, through the funding of the PhD studies of the corresponding author.

The authors have no conflict of interest to declare.

Literature Cited

1. Tanzeglock T, Soos M, Stephanopoulos G, Morbidelli M. Induction of mammalian cell death by simple shear and extensional flows. *Biotechnology and Bioengineering*. 2009;104(2):360–370.
2. Neunstoecklin B, Stettler M, Solacroup T, Broly H, Morbidelli M, Soos M. Determination of the maximum operating range of hydrodynamic stress in mammalian cell culture. *Journal of Biotechnology*. 2015;194:100–109.
3. Schügerl K, Kretzmer G, Henzler HJ, Kieran PM, Kretzmer G, MacLoughlin PE, Malone DM, Schumann W, Shamlou PA, Yim SS, Scheper T, Babel W, Blanch HW, Cooney CL, Endo I, Enfors SO, Eriksson KEL, Fiechter A, Hoare M, Mattiasson B, Rehm HJ, Rogers PL, Sahm H, Schügerl K, Stephanopoulos G, Tsao GT, Venkat K, Villadsen J, Stockar U, Wandrey C. , eds.*Influence of Stress on Cell Growth and Product Formation*;67 of

Advances in Biochemical Engineering/Biotechnology. Berlin, Heidelberg: Springer Berlin Heidelberg 2000 Available at: <http://link.springer.com/10.1007/3-540-47865-5>.

4. Chen HC, Lee HP, Sung ML, Liao CJ, Hu YC. A Novel Rotating-Shaft Bioreactor for Two-Phase Cultivation of Tissue-Engineered Cartilage. *Biotechnology Progress*. 2004;20(6):1802–1809.
5. Liu Y, Li F, Hu W, Wiltberger K, Ryll T. Effects of bubble–liquid two-phase turbulent hydrodynamics on cell damage in sparged bioreactor. *Biotechnology Progress*. 2014;30(1):48–58.
6. Li F, Vijayasankaran N, Shen AY, Kiss R, Amanullah A. Cell culture processes for monoclonal antibody production. *MAbs*. 2010;2(5):466–477.
7. Bekard IB, Asimakis P, Bertolini J, Dunstan DE. The effects of shear flow on protein structure and function. *Biopolymers*. 2011;95(11):733–745.
8. Barnes JM, Nauseef JT, Henry MD. Resistance to Fluid Shear Stress Is a Conserved Biophysical Property of Malignant Cells. *PLOS ONE*. 2012;7(12):e50973.
9. Li W, Mao S, Khan M, Zhang Q, Huang Q, Feng S, Lin JM. Responses of Cellular Adhesion Strength and Stiffness to Fluid Shear Stress during Tumor Cell Rolling Motion. *ACS Sens.* 2019;4(6):1710–1715.
10. Kim SW, Ehrman J, Ahn MR, Kondo J, Lopez A, Oh Y, Kim H, Crawley S, Goldenring J, Tyska M, Rericha E, Lau K. Shear stress induces non-canonical autophagic flux in intestinal epithelial monolayers. *Molecular Biology of the Cell*. 2017;28:mbc.E17–01.
11. Latz MI, Juhl AR, Ahmed AM, Elghobashi SE, Rohr J. Hydrodynamic stimulation of dinoflagellate bioluminescence: a computational and experimental study. *Journal of Experimental Biology*. 2004;207(11):1941–1951.
12. Borys BS, Dang T, So T, Rohani L, Revay T, Walsh T, Thompson M, Argiropoulos B, Rancourt DE, Jung S, Hashimura Y, Lee B, Kallos MS. Overcoming bioprocess bottlenecks in the large-scale expansion of high-quality hiPSC aggregates in vertical-wheel stirred suspension bioreactors. *Stem Cell Research & Therapy*. 2021;12(1):55.

13. Verma R, Mehan L, Kumar R, Kumar A, Srivastava A. Computational fluid dynamic analysis of hydrodynamic shear stress generated by different impeller combinations in stirred bioreactor. *Biochemical Engineering Journal*. 2019;151:107312.
14. Zhan C, Bidkhorji G, Schwarz H, Malm M, Mebrahtu A, Field R, Sellick C, Hatton D, Varley P, Mardinoglu A, Rockberg J, Chotteau V. Low Shear Stress Increases Recombinant Protein Production and High Shear Stress Increases Apoptosis in Human Cells. *iScience*. 2020;23(11):101653.
15. Barbosa MJ, Albrecht M, Wijffels RH. Hydrodynamic stress and lethal events in sparged microalgae cultures. *Biotechnology and Bioengineering*. 2003;83(1):112–120.
16. Blaser S. *The hydrodynamical effect of vorticity and strain on the mechanical stability of flocs*. PhD thesis. ETH Zurich; 1998.
17. Li C, Teng X, Peng H, Yi X, Zhuang Y, Zhang S, Xia J. Novel scale-up strategy based on three-dimensional shear space for animal cell culture. *Chemical Engineering Science*. 2020;212:115329.
18. Garcia-Ochoa F, Gomez E, Alcon A, Santos VE. The effect of hydrodynamic stress on the growth of *Xanthomonas campestris* cultures in a stirred and sparged tank bioreactor. *Bioprocess Biosyst Eng*. 2013;36(7):911–925.
19. Cherry RS. Animal cells in turbulent fluids: Details of the physical stimulus and the biological response. *Biotechnology Advances*. 1993;11(2):279–299.
20. Šrom O, Trávníková V, Wutz J, Kuschel M, Unsoeld A, Wucherpfennig T, Šoóš M. Characterization of hydrodynamic stress in ambr250® bioreactor system and its impact on mammalian cell culture. *Biochemical Engineering Journal*. 2022;177:108240.
21. Wollny S. *Experimentelle und numerische Untersuchungen zur Partikelbeanspruchung in gerührten (Bio-)Reaktoren*. PhD thesis. Technische Universität Berlin; 2010.
22. Kreitmayer D, Gopireddy SR, Matsuura T, Aki Y, Katayama Y, Sawada T, Kakihara H, Nonaka K, Profitlich T, Urbanetz NA, Gutheil E. Numerical and Experimental In-

- vestigation of the Hydrodynamics in the Single-Use Bioreactor Mobius® CellReady 3 L. *Bioengineering*. 2022;9(5):206.
23. Gurtin ME, Fried E, Anand L. The Mechanics and Thermodynamics of Continua. 2010:718.
 24. Ferziger JH, Perić M. *Computational methods for fluid dynamics*. Berlin ; New York: Springer (3rd edition). 2002.
 25. Bird RB, Stewart WE, Lightfoot EN. *Transport Phenomena*. New York: John Wiley & Sons, Inc. (2nd edition). 2006.
 26. Mollet M, Ma N, Zhao Y, Brodkey R, Taticek R, Chalmers JJ. Bioprocess Equipment: Characterization of Energy Dissipation Rate and Its Potential to Damage Cells. *Biotechnology Progress*. 2004;20(5):1437–1448.
 27. Pope SB. *Turbulent flows*. Cambridge ; New York: Cambridge University Press 2000.
 28. Kaiser S. *Characterization and optimization of single-use bioreactors and biopharmaceutical production processes using computational fluid dynamics*. PhD thesis. Technische Universität Berlin; 2014.
 29. Zhu L, Song B, Wang Z. Developing an orbitally shaken bioreactor featuring a hollow cylinder vessel wall. *Journal of Chemical Technology & Biotechnology*. 2019;94(7):2212–2218.
 30. Zhan C, Hagrot E, Brandt L, Chotteau V. Study of hydrodynamics in wave bioreactors by computational fluid dynamics reveals a resonance phenomenon. *Chemical Engineering Science*. 2019;193:53–65.
 31. Kaiser SC, Löffelholz C, Werner S, Eibl D. CFD for Characterizing Standard and Single-use Stirred Cell Culture Bioreactors. *Computational Fluid Dynamics Technologies and Applications*. 2011.
 32. Langer G, Deppe A. Zum Verständnis der hydrodynamischen Beanspruchung von Partikeln in turbulenten Rührerströmungen. *Chemie Ingenieur Technik*. 2000:11.

33. Werner S, Kaiser SC, Kraume M, Eibl D. Computational fluid dynamics as a modern tool for engineering characterization of bioreactors. *Pharmaceutical Bioprocessing*. 2014;2(1):85–99.
34. Kaiser SC, Eibl R, Eibl D. Engineering characteristics of a single-use stirred bioreactor at bench-scale: The Mobius CellReady 3L bioreactor as a case study. *Engineering in Life Sciences*. 2011;11(4):359–368.
35. Hellevik LR. *Cardiovascular biomechanics* . 2018 Available at: <https://folk.ntnu.no/leifh/teaching/tkt4150/main.pdf>.
36. Sorg R, Tanzeglock T, Soos M, Morbidelli M, Périlleux A, Solacroup T, Broly H. Minimizing hydrodynamic stress in mammalian cell culture through the lobed Taylor-Couette bioreactor. *Biotechnology Journal*. 2011;6(12):1504–1515.
37. Malvern L. *Introduction to the Mechanics of a Continuous Medium*. Englewood Cliffs, N.J: Pearson College Div (1st edition). 1969.
38. Taylor GI. The viscosity of a fluid containing small drops of another fluid. *Proceedings of the Royal Society of London. Series A, Containing Papers of a Mathematical and Physical Character*. 1932;138(834):41–48.
39. Wengeler R, Nirschl H. Turbulent hydrodynamic stress induced dispersion and fragmentation of nanoscale agglomerates. *Journal of Colloid and Interface Science*. 2007;306(2):262–273.
40. Wang G, Yang F, Wu K, Ma Y, Peng C, Liu T, Wang LP. Estimation of the dissipation rate of turbulent kinetic energy: A review. *Chemical Engineering Science*. 2021;229:116133.
41. Morshed KN, Bark Jr. D, Forleo M, Dasi LP. Theory to Predict Shear Stress on Cells in Turbulent Blood Flow. *PLoS One*. 2014;9(8):e105357.
42. Villiger TK, Neunstoecklin B, Karst DJ, Lucas E, Stettler M, Broly H, Morbidelli M, Soos M. Experimental and CFD physical characterization of animal cell bioreactors: From micro- to production scale. *Biochemical Engineering Journal*. 2018;131:84–94.

43. Kaya U, Gopireddy S, Urbanetz N, Nopens I, Verwaeren J. Predicting the hydrodynamic properties of a bioreactor: Conditional density estimation as a surrogate model for CFD simulations. *Chemical Engineering Research and Design*. 2022;182:342–359.